Dose-Response:
An International Journal
April-June 2018:1-12

DOI: 10.1177/1559325818778633
journals.sagepub.com/home/dos
SAGE

Comparative Profiling of MicroRNAs Reveals the Underlying Toxicological Mechanism in Mice Testis Following Carbon Ion Radiation

Yuxuan He[1], Yong Zhang[1], Hongyan Li[2], Hong Zhang[2], Zongshuai Li[1], Longfei Xiao[1], Junjie Hu[1], Youji Ma[1], Quanwei Zhang[1], and Xingxu Zhao[1]

Abstract

This study investigated the toxicity of heavy ion radiation to mice testis by microRNA (miRNA) sequencing and bioinformatics analyses. Testicular indices and histology were measured following enterocoelia irradiation with a 2 Gy carbon ion beam, with the testes exhibiting the most serious injuries at 4 weeks after carbon ion radiation (CIR) exposure. Illumina sequencing technology was used to sequence small RNA libraries of the control and irradiated groups at 4 weeks after CIR. Gene Ontology and Kyoto Encyclopedia of Genes and Genomes pathway analyses implicated differential miRNAs in the regulation of target genes involved in metabolism, development, and reproduction. Here, 8 miRNAs, including miR-34c-5p, miR-138, and 6 let-7 miRNA family members previously reported in testis after radiation, were analyzed by quantitative reverse transcription-polymerase chain reaction (qRT-PCR) to validate miRNA sequencing data. The differentially expressed miRNAs described here provided a novel perspective for the role of miRNAs in testis toxicity following CIR.

Keywords

heavy ion radiation, miRNAs, testis

Introduction

Testis is the key organ involved in maintaining male fertility through testosterone synthesis and production of the male gamete.[1] Additionally, spermatogenesis in the testis occurs via germ cell differentiation at different stages of development.[2] Testis is also among the most radiosensitive organs and can be significantly impaired by ionizing radiation (IR) exposure.[3] The toxic effects of IR interfere with normal spermatogenesis, affecting the proliferation and differentiation of spermatogenic cells, which ultimately leads to cell mutagenesis or apoptosis and results in reduced sperm counts and defective sperm production.[4] Cancer treatment by radiation or exposure to IR usually results in temporary destruction or complete cessation of spermatogenesis.[5,6] Therefore, temporary or permanent infertility is a common problem associated with radiation, especially in young men.[7] In recent years, heavy ion radiation has been used in clinical radiotherapy; however, high linear energy transfer (LET) heavy ions have a higher likelihood of damaging cells when compared to low-LET radiation, including X- or γ-rays. Therefore, it is important to investigate the mechanisms underlying injuries acquired from testis exposure to high-LET radiation.[8,9]

MicroRNAs (miRNAs) are produced by genomic transcription[10] and regulate the expression of multiple genes by cleavage or translation inhibition.[11] Investigation of functions related to miRNAs and their regulatory roles contributed to the discovery of information delivery patterns and miRNA-mediated gene regulatory networks, which further clarified different aspects of biological activities.[12] The study of miRNA

[1] College of Veterinary Medicine, Gansu Agricultural University, Lanzhou, China
[2] Department of Radiation Medicine, Institute of Modern Physics, Chinese Academy of Sciences, Lanzhou, China

Received 01 December 2017; received revised 13 February 2018; accepted 13 February 2018

Corresponding Author:
Xingxu Zhao, College of Veterinary Medicine, Gansu Agricultural University, Lanzhou 730070, China.
Email: zhaoxx@gsau.edu.cn

function in testes allowed insight into human disease mechanisms. Tang et al discovered that upregulation of miR-210 is associated with spermatogenesis by targeting insulin-like growth factor (IGF) 2 in male infertility,[13] and Noveski et al reported that the expression of 5 miRNAs (hsa-miR-34b, hsa-miR-449b, hsa-miR-517c, hsa-miR-181c, and hsa-miR-605) was associated with impaired spermatogenesis in patients.[14]

In this study, we determined differential expression profiles for miRNAs based on miRNA-seq analyses following carbon ion radiation (CIR) exposure in mouse testis and investigated the underlying toxicological mechanisms. These results provided insight for evaluating environmental or clinical risks of CIR exposure.

Materials and Methods

Animals and Irradiation Procedure

Healthy male Swiss-Webster mice were purchased from Lanzhou Medical College (Lanzhou, China); the mice aged 4 weeks and weighing 14 to 18 g. Animals were randomly assigned to a control (CK) and CIR (2 Gy) groups ($n = 15$ in each group) and were acclimatized to the same laboratory conditions for 1 week before use and were housed in a conventional animal facility at $22°C \pm 2°C$, $60\% \pm 10\%$ humidity, and a 12-hour light –12-hour dark photoperiod, with 3 mice per cage. All experiments were approved by the Institutional Animal Care Committee. Five-week-old mice were enterocoelia irradiated with a 2 Gy carbon-ion beam at 250 MeV/U and 31.3 keV/μm (at the beam entrance), to give a dose of approximately 0.5 Gy/min, at the Heavy Ion Research Facility in Lanzhou (Institute of Modern Physics, Chinese Academy of Sciences, Lanzhou, China).[15]

Testes Were Weighed, Fixed, and Histopathologic Observation

Five mice from each group were used at 1, 4, and 7 weeks after CIR and were killed by cervical dislocation. The testes of each mouse were taken out and connective tissues were removed. Left testes were fixed in 4% paraformaldehyde solution (4 g paraformaldehyde in 100 mL phosphate buffer saline) and embedded in paraffin blocks, and right testes were frozen immediately in liquid nitrogen and stored at $-80°C$ until analysis.[16]

Histopathologic Observation and Observation of Spermatogenic Cells Apoptosis

The fixed tissues were thoroughly washed in 0.01 phosphate buffer (pH 7.4), dehydrated in graded ethanol, toluene-cleared, and embedded in paraffin. Paraffin sections of testis and cauda epididymis were cut at 5 μm, mounted on slides, and stained with hematoxylin and eosin and observed under a light microscope (Nikon 80i; Nikon, Japan).[6] The in situ Cell Death Detection horseradish peroxidase Kit (Roche, Mannheim, Germany) was used to carry out the terminal 2′-deoxyuridine 5′-triphosphate nick end-labeling (TUNEL) assay. Briefly, paraffin blocks of testis material were cut into 4-μm thick sections and treated with 20 mg/mL proteinase K solution for 20 minutes at 37°C. The TUNEL reaction was then performed in TdT buffer in the presence of dUTP-biotin for 60 minutes at 37°C and then incubated with the secondary antifluorescein-POD-conjugate for 30 minutes. The signal was visualized using diaminobenzidine. Sections were then counterstained with hematoxylin, dehydrated, cleaned, mounted, and observed under a light microscope (Axio10, Zeiss, Germany).

Total RNA Extraction for Testis

The total RNA of testes at 4 weeks after CIR was isolated from the strain using the Trizol reagent according to manufacturer's instructions (Invitrogen, Carlsbad, California). An additional DNase I digestion step was performed to ensure that the samples were not contaminated with genomic DNA. RNA purity was assessed using the Nanodrop-2000. Each RNA sample had an A260:A280 ratio above 1.8 and A260:A230 ratio above 2.2.

Small RNA Library Construction, Sequencing, and Data Processing

Approximately 1 μg of total RNA was used to prepare small RNA library according to protocol of NEBNext Small RNA Library Prep Set for Illumina. And then, we performed the single-end sequencing (50 bp) on an Illumina Hiseq2500 at ORI-GENE (Beijing, China) following the vendor's recommended protocol.

Raw reads were checked for potential sequencing issues and contaminants using FastQC. Adapter sequences, primers, Ns, polyA/polyT, and reads with quality scores below 20 were trimmed. Reads with a length <10 nt and >34 nt were discarded. The clean reads that were obtained were compared with the Rfam10.1 database using BLAST to annotate the sRNA sequences. The clean reads were aligned against the miRNA precursor/mature miRNA of Homo sapiens and other species in miRBase 20.0 (http://www.mirbase.org/) to identify known miRNAs. The unannotated sequences were mapped to the human genome to analyze their expression and distribution in the genome and then used to predict potential novel miRNA candidates by Mireap (http://sourceforge.net/projects/mireap/). The read counts of each known miRNA were then normalized to the total counts of sequence reads mapped to the miRBase version 20.0 database and are presented as reads per million mapped reads. MicroRNA differential expression based on normalized deep-sequencing counts was analyzed by selectively using permutation test based on the experiments design. The P value was identified by the false discovery rate (FDR), which defines the Benjamini-Hochberg correction to determine different expression levels between the 2 groups. A criterion of $|\log2(\text{fold-change})| \geq 1$ and P value <.05 between the 2 groups was used to identify differentially expressed miRNAs.[17]

Prediction of Target Genes and Gene Ontology Analysis

Potential targets of all the miRNAs identified were predicted using psRNATarget (http://plantgrn.noble.org/psRNATarget/) with default parameter settings. Since genome sequence was unavailable for *Mus musculus*, we used the total expressed sequence tags of mouse as the pool for the putative miRNA targets prediction. The target genes were aligned to the Cluster of Orthologous Groups and Kyoto Encyclopedia of Genes and Genomes (KEGG) databases to predict and classify possible functions. Functional annotation was also assigned according to the Gene Ontology (GO) database (http://www.geneontology.org/). The GO enrichment analysis was performed for target genes of thermogenesis-related miRNAs using BiNGO.[18]

Real-Time Quantitative Polymerase Chain Reaction

Total RNA was extracted from the testis by using Trizol reagent according to the manufacturer's protocol (Invitrogen, Life Technologies, Carlsbad, CA, USA). Quantitative reverse transcription-polymerase chain reaction (qRT-PCR) analyses for miRNAs identified by miRNA sequencing were performed using PrimeScript RT Reagent Kit with gDNA Eraser (Takara-Bio, Otsu, Japan). Reverse transcription reactions were performed at the following parameters: 42°C, 5 minutes; 42°C (miRNA), 30 minutes; and 85°C, 2 minutes. The PCR reactions were performed at the following parameters: 95°C for 2 minutes followed by 40 cycles of 95°C, 15 seconds and 59°C, 30 seconds. A U6 small nuclear RNA was used as endogenous control for data normalization of miRNAs. U6: forward primer: forward 5′-CGCTTCGGCAGCACATATAC-3′; reverse 5′-AAATATGGAACGCTTCACGA-3′. The universal primer of miRNA antisense strand: R primer: CCAGTGCAGGGTCC GAGGTATT. Relative expression was calculated by the comparative threshold cycle method. The sequences of primers used for reverse transcription and qRT-PCR were purchased from RiboBio Company (Guangzhou, China).[19,20]

Statistical Analyses

All values are presented as mean ± standard error of mean (SEM). For small RNA-sequencing data, the threshold values we used to identify the differentially expressed miRNAs are |log2 (fold-change)| ≥ 1, and P value <.05. For RT-PCR data, statistical analysis was performed in Statistical Package for Social Sciences 16.0. The fold changes were calculated through relative quantification with $2^{-\Delta\Delta CT}$. $P < .05$ was considered statistically significant.

Results

The Effect of CIR on Histology and Spermatogenic Cell Apoptosis of Testis

To investigate the intrinsic causes of testes weight reduction, we compared testicular histological changes and rates of spermatogenic cell apoptosis at 1, 4, and 7 weeks after CIR exposure. Photomicrographs of testis sections in each group are shown in Figure 1. The control group exhibited smooth seminiferous tubules and regular arrangement of all spermatogenic cells. Compared to controls, at 1 week, the number of vacuoles increased (asterisks), and spermatogenic cells were severely disorganized. At 4 weeks, spermatogenic cells were severely disorganized and the thickness of the epithelium decreased. At 7 weeks, spermatogenic cells gradually returned to normal arrangements with the exception of numerous vacuoles.

Rates of apoptosis in spermatogenic cells following CIR were examined by terminal deoxynucleotidyl transferase dUTP nick-end labeling assay (Figure 2). The control group showed a normal apoptotic profile, with almost no positively stained (apoptotic) cells in seminiferous tubules. By contrast, additional spermatogenic cells appeared in the CIR group at 1 and 4 weeks, with the most severe damage observed in spermatogonia and primary spermatocytes. However, at 7 weeks, there were no significant differences between control and CIR groups.

Screening of Differentially Expressed miRNAs

We used Illumina sequencing technology to sequence small RNA libraries of the control and irradiated groups. After filtering out adapter and low-quality sequences and removing ribosomal, transfer, and small nucleolar RNAs and repeat regions, we identified mature miRNAs using BLAST to compare miRNA sequences from the miRBase database with miRNA sequences from other species. Our results indicated that the sequences derived from this study were known according to sequencing data related to mature miRNAs.

We identified mature miRNAs in the sequencing data by means of database comparison and bioinformatics prediction and based on structural analysis to ensure consistency with known miRNA structures and mechanisms. MicroRNA sequences not identified in current databases were defined as novel miRNAs. For sequences not identified as known miRNAs, they were first mapped to the reference genome using Bowtie2 (http://bowtie-bio.sourceforge.net/bowtie2/index.shtml), and the MIREAP program (https://sourceforge.net/projects/mireap/) was used to predict novel miRNAs based on localization results. A total of 8508 known mature miRNAs and 105 novel miRNAs were identified in the control and CIR groups, respectively. The length distribution of the sequences identified as mature miRNAs (1432 miRNAs) was mainly in the range of 21 to 23 nt, exhibiting a typical normal distribution and with 22 nt accounting for the highest proportion (41.8%; Figure 3A). Sequences in ranges of 22 to 23 nt were in line with typical characteristics associated with Dicer enzyme cleavage. The specificity of Dicer-cleavage sites results in sequences beginning with a uridine base, giving these sequences stronger preference for development from precursor to mature miRNA. We analyzed the base distribution of each locus for all miRNA sequences (Figure 3B) to derive profiles of identified miRNAs in different species (Figure 3C) and calculated the

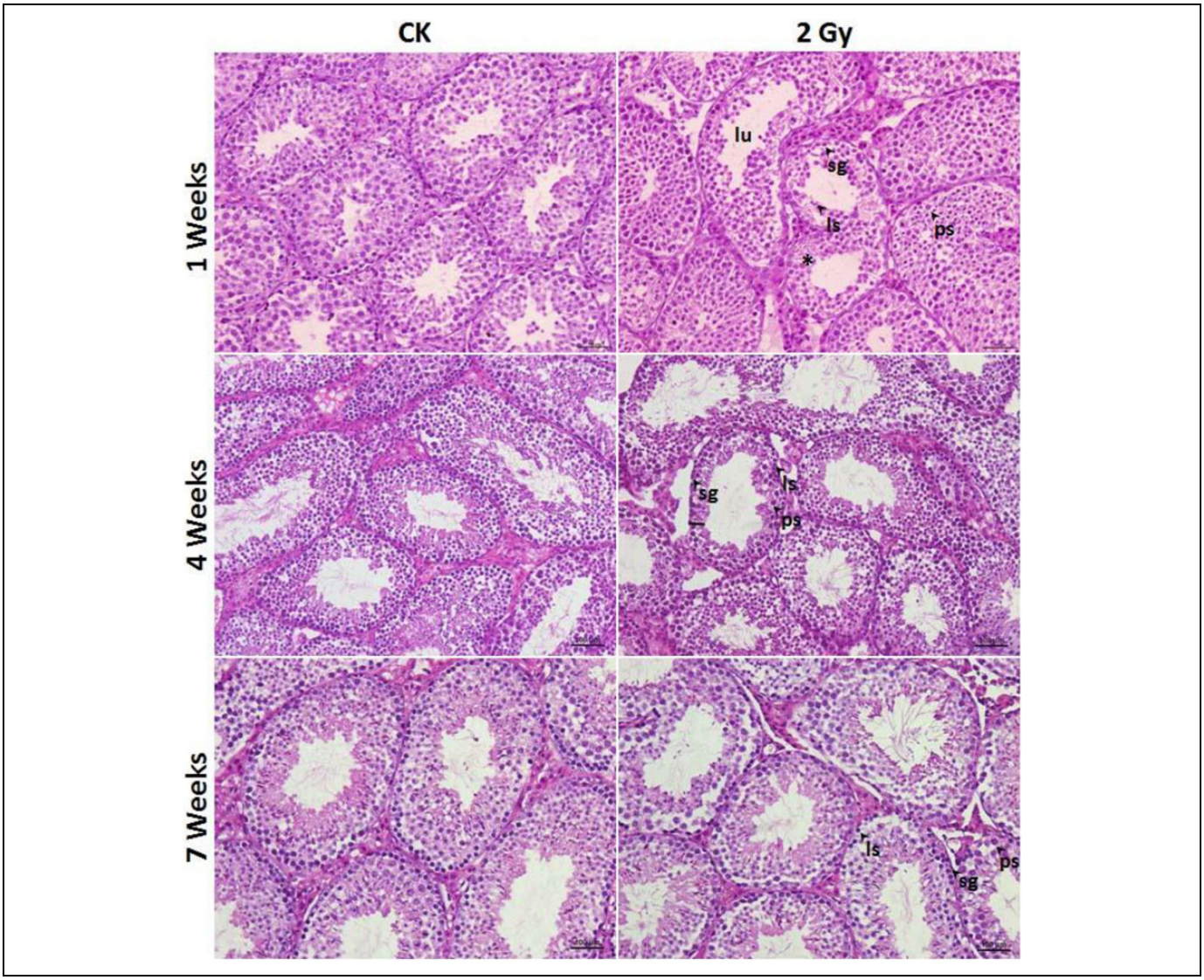

Figure 1. Histological examination of testis in mice at 1, 4, and 7 weeks after carbon ion radiation (CIR). Photomicrographs of sections stained with hematoxylin and eosin (H&E; magnification × 200; scale bar = 100 μm). Arrows indicate spermatogenic cells in the seminiferous tubule, severe degeneration of spermatogenic cells in the seminiferous tubule (*). CK indicates control; lu, lumen; ls, leptotene-stage spermatocyte; ps, pachytene spermatocyte; sg, spermatogonia.

reads per million for all miRNAs in individual testis of control and irradiated mice determine similarities in miRNA expression levels between the 2 groups (Figure 3D).

Among the known miRNAs, there were 70 differentially expressed ($|\log2(\text{fold-change})| \geq 1$ and P value $<.05$) between the control and CIR groups. When compared to controls, 56 miRNAs were upregulated and 14 were downregulated in the CIR group. Details for the downregulated miRNAs are listed in Table 1, and those for the upregulated miRNAs are listed in Table 2. A volcano plot (Figure 4) illustrates the height differential related to miRNAs expression, a criterion of $|\log2(\text{fold-change})| \geq 1$ and P value $<.05$ between the 2 groups was used to identify differentially expressed miRNAs. The miRNAs expression profiles heatmap shown in Figure 5 was constructed using mirPathv.3 Online Software (http://snf-515788.vm.okeanos.grnet.gr/dianauniverse/index.php?r=mirpath).

Functional Analysis of Differentially Expressed miRNAs

The GO threshold of significance was defined as $P < .001$ and an FDR $< .05$. A total of 539 GO-enriched terms were identified describing predicted functions of overexpressed miRNAs and included positive regulation of transcription from the RNA polymerase II promoter, protein homodimerization activity, and positive regulation of transcription from a DNA template. By contrast, 527 GO terms associated with downregulated miRNAs included protein homodimerization activity, poly(A) RNA-binding, and positive regulation of transcription from RNA polymerase II promoter. Significant GO-enriched terms

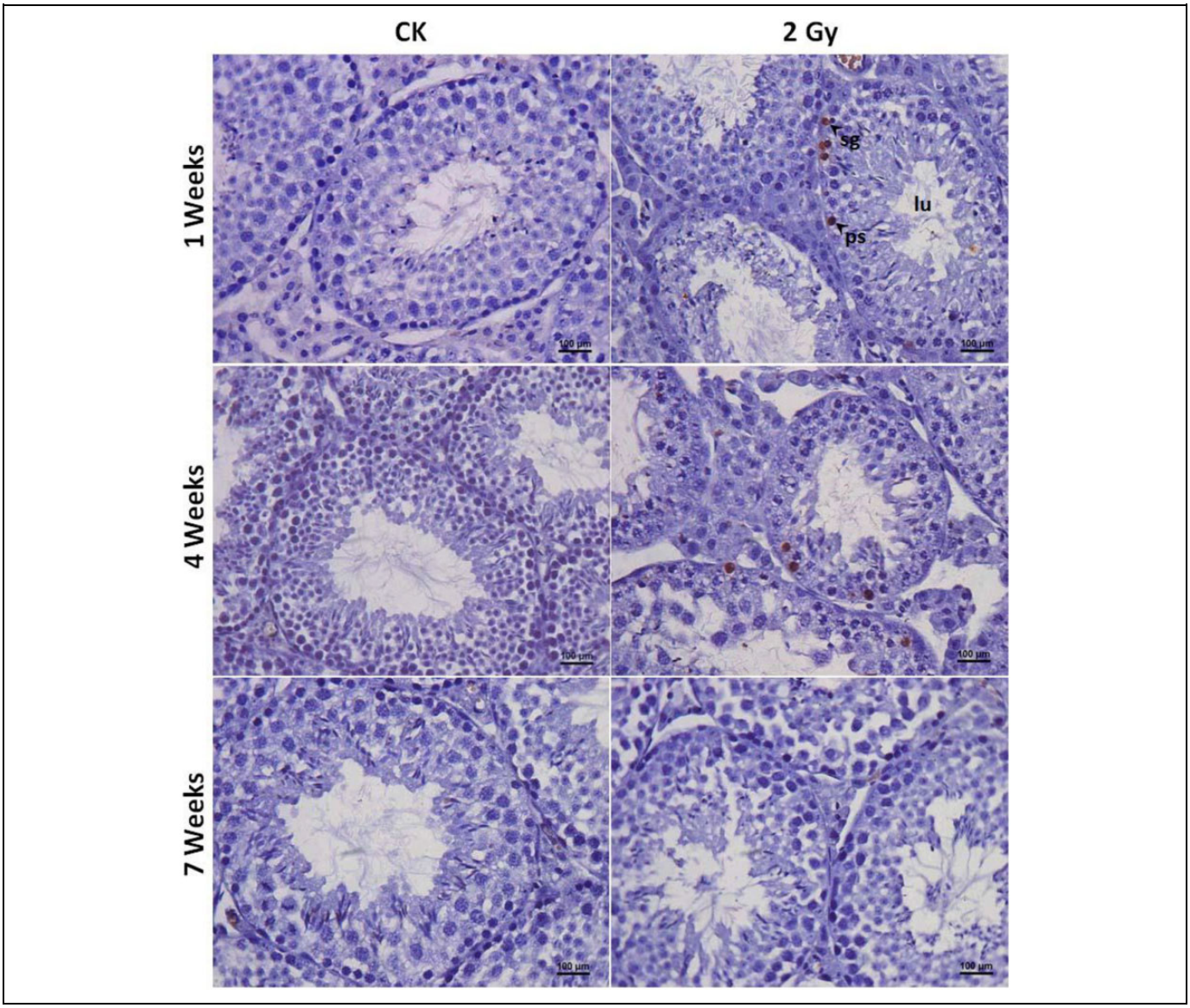

Figure 2. Photomicrographs of apoptotic spermatogenic cells in mice at 1, 4, and 7 weeks after carbon ion radiation (CIR; magnification ×400; scale bar = 100 μm). Arrows indicate terminal dUTP nick end-labeling (TUNEL)-positive cells in the seminiferous tubule. CK indicates control; lu, lumen; ps, pachytene spermatocyte.

are presented in Figure 6. Based on GO-enrichment analyses, the target gene of the differentially expressed miRNAs were enriched.

Prediction of Target Genes of Differentially Expressed miRNAs

The target genes of the 70 differentially expressed miRNAs were predicted using TargetScan software (http://www.targetscan.org/mouse). The 56 upregulated miRNAs had 15 838 potential target genes, with 539 significant GO terms describing predicted target gene functions. The significant GO-enriched terms for the target genes of upregulated miRNAs are presented in Figure 7A. The 14 downregulated miRNAs had 14 519 potential target genes, with 527 significant GO terms describing predicted target gene functions. The significant GO-enriched terms for the target genes of downregulated miRNAs are presented in Figure 7B. These GO terms represented a wide range of biological processes, including metabolic, single organism, organelle, cellular, binding, cell, cell components. Based on KEGG analyses, KEGG pathway analysis of the target genes indicated 175 pathways involving target genes of the upregulated miRNAs and 163 pathways involving target genes of the downregulated miRNAs, including MAPK, Ras, cancer pathways, ubiquitin-mediated proteolysis, and apoptosis. The significant functions and pathways associated with the differentially expressed miRNA and their target genes are presented in Figure 7.

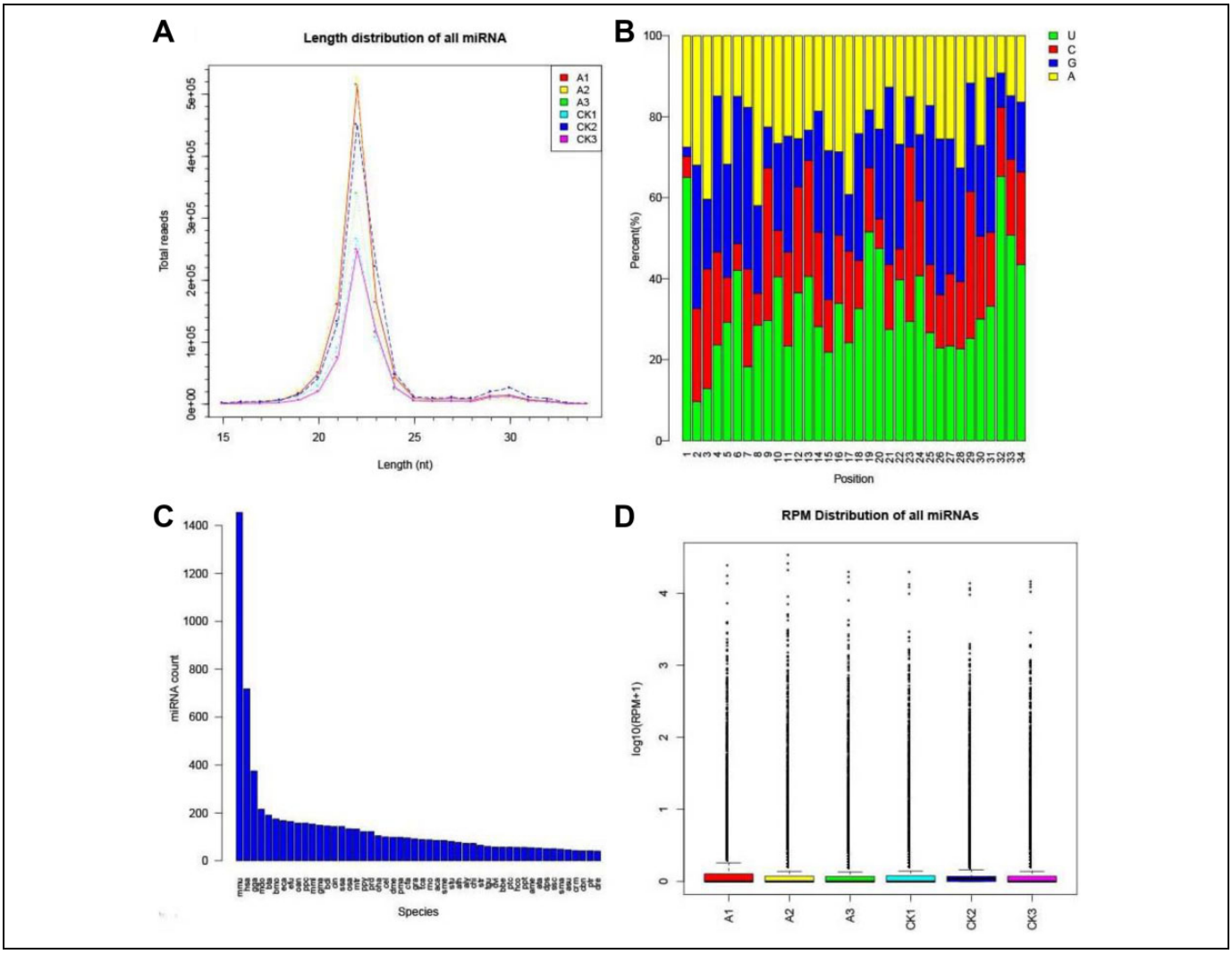

Figure 3. The basic information of microRNAs (miRNAs) in mice testis at 4 weeks after carbon ion radiation (CIR). The length distribution of the sequences identified as mature miRNAs (A); CK, control; A, 2 Gy CIR exposure. The base distribution of each locus for all miRNA sequences (B). The profiles of identified miRNAs in different species (C). The reads per million for all miRNAs in individual testis of control (CK) and irradiated mice (A) determine similarities in miRNA expression levels between the 2 groups (D).

Table 1. The Details for the Downregulated microRNAs (miRNAs) in Mice Testis at 4 Weeks After CIR.

miRNA	miRNA Sequence	Fold Change (A/CK)	Log_2 Fold Change	*P* Value
aca-miR-34b-3p_R15-1L22	TATGATCTAACCTGTATTCTTGCTGATT	0.426477	−1.22946	.042665
bdi-miR169l_R1-17L21	TAGCCAAGGATGAATTGATTAGCTTATC	0	None	.001283
cel-miR-255-5p_R15-1L22	TGAAAATTCGATTAGACAAAGATTTCTTACA	0.299071	−1.74144	.021688
chi-miR-483_R7-21L22	TAAGAAGAGTCACTTCTCCTCCCGTCTTCCC	0.295917	−1.75673	.006581
efu-miR-9189e_R18-4L24	TTCCAGGGAACCCGGGTTCAATTCCCAGC	0.462986	−1.11096	.046978
efu-miR-9239_R20-6L22	TACCTTCGTGGAGCTACAAAGTGATACTATGC	0.452137	−1.14517	.037228
efu-miR-9360_R18-4L18	TGATGAACTCCTGCAGGGCCCCAGC	0.479584	−1.06015	.044845
gra-miR8672_R21-7L24	ATCTATCTTGAAGACTTTCATACAATCATT	0.424297	−1.23685	.041653
mdo-miR-7344-5p_R19-5L22	TGTGGATGGCACTCAAGGGAAGAGCAATC	0.375755	−1.41214	.020257
mmu-miR-138-5p_R1-23L23	AGCTGGTGTTGTGAATCAGGCCGTT	0.485429	−1.04267	.008146
mmu-miR-5623-5p_R19-4L24	TCGCTCTGACTTGCCAGCTGTATGGCTTC	0.299939	−1.73726	.044782
mse-miR-34_R2-23L23_19G-A	AGGCAGTGTGGTTAGCTGATTGT	0.438542	−1.18921	.028403
oha-miR-34c-5p_8G-T	AGGCAGTTTAGTTAGCTGATTGT	0.289266	−1.78953	.006227
str-miR-34b-5p_R5-22L22	AGGAAGTGTAGTTAGCTGGTTGT	0.325623	−1.61873	.007615

Abbreviations: A, 2 Gy CIR exposure; CIR, carbon ion radiation; CK, control; miRNA, microRNA.

Table 2. The Details for the Upregulated miRNAs in Mice Testis at 4 Weeks After CIR.

miRNA	miRNA Sequence	Fold Change (A/CK)	Log_2 Fold Change	*P* Value
api-let-7_R1-21L21	TGAGGTAGTTGGTTGTATAGTC	2.558611	1.355361	.015772
bta-miR-2340_R6-22L22	TCCCTGGTGGTCTTGTGGTTAGGATTCGGCGCTC	3.11591	1.639654	.046913
chi-miR-1248-5p_R1-15L20	ACCTTCTTGTATAAG	8.075667	3.013581	.042288
dre-miR-199-3-3p_R1-21L21	ACAGTAGTCCGCACATTGGTTA	2.905431	1.538752	.015805
dre-miR-30a-5p_R4-22L22	TGGAAACATTCCCGACTGGAAGC	3.272599	1.710437	.047175
hhi-let-7j_R1-22L22	TGAGGTAGTTGTTTGTACAGTTT	2.338941	1.225856	.006712
lva-let-7-5p	TGAGGTAGTAGGTTATATAGTT	2.582792	1.368931	.028594
mdo-miR-7334-5p_R3-17L27	AAGCTGTGATGAATTTGAATCCACTGATCTTCCG	2.377797	1.249625	.030171
mmu-let-7a-5p_R1-22L22	TGAGGTAGTAGGTTGTATAGTTC	2.122323	1.085644	.045588
mmu-let-7b-5p_R1-20L22	TGAGGTAGTAGGTTGTGTGGC	2.120538	1.08443	.048089
mmu-let-7c-5p_R4-21L22	TGTGGTAGTAGGTTGTATGGTA	2.27431	1.185429	.044656
mmu-let-7e-5p_R1-21L22	TGAGGTAGGAGGTTGTATAGTC	2.184751	1.127469	.015838
mmu-let-7f-5p_R1-22L22	TGAGGTAGTAGATTGTATAGTTA	2.650922	1.406494	.032903
mmu-let-7i-5p_R4-21L22	TGGGGTAGTAGTTTGTGCTGTC	2.450948	1.29334	.039731
mmu-miR-10b-3p_R1-20L22	ACAGATTCGATTCTAGGGGAAC	2.188405	1.12988	.048433
mmu-miR-1198-5p_R4-22L22	TAGGTGTTCCTGGCTGGCTTGG	2.425107	1.278048	.029492
mmu-miR-125b-2-3p_R1-19L22	ACAAGTCAGGTTCTTGGGA	2.183858	1.126879	.036914
mmu-miR-129-5p_R4-21L21	CTGTTTGCGGTCTGGGCTTGCA	2.637509	1.399176	.048279
mmu-miR-145a-3p_R1-20L22	ATTCCTGGAAATACTGTTCTAT	2.611941	1.385122	.038685
mmu-miR-181b-5p_R1-19L23	AACATTCATTGCTGTCGGTA	2.080111	1.056661	.006614
mmu-miR-1843b-5p_R1-20L21	ATGGAGGTCTCTGTCTGACTG	2.03783	1.027034	.043665
mmu-miR-187-3p_R1-21L22	TCGTGTCTTGTGTTGCAGCCGTT	6.448071	2.688868	.010346
mmu-miR-1947-5p_R1-22L22	AGGACGAGCTAGCTGAGTGCTGT	2.134532	1.09392	.006326
mmu-miR-199b-3p_R5-21L22	ACAATAGTCTGCACATTGGTT	2.364176	1.241337	.031889
mmu-miR-1a-3p_17A-C	TGGAATGTAAAGAAGTCTGTAT	2.497655	1.320574	.000983
mmu-miR-200a-3p_R1-21L22	TAACACTGTCTGGTAACGATGC	2.326216	1.217985	.006096
mmu-miR-200b-3p_R1-22L22	TAATACTGCCTGGTAATGATGACA	3.100953	1.632711	.038718
mmu-miR-214-5p_R1-21L22	TGCCTGTCTACACTTGCTGTG	2.023334	1.016734	.016391
mmu-miR-221-5p_R1-21L26	ACCTGGCATACAATGTAGATT	2.096145	1.067738	.046504
mmu-miR-27a-5p_R5-21L22	AGGACTTAGCTGCTTGTGAGC	3.425775	1.77643	.032381
mmu-miR-27b-5p_R1-22L22	CAGAGCTTAGCTGATTGGTGAACA	2.94128	1.556444	.046567
mmu-miR-292a-5p_R1-20L22	ACTCAAACTGGGGGCTCTTT	2.034526	1.024693	.033673
mmu-miR-3071-3p_R22-2L22	AGGACTCCATTTGTTTTGATGA	6.108276	2.610765	.00203
mmu-miR-322-3p_R1-19L21	CAAAACATGAAGCGCTGCAACG	2.433433	1.282993	.016092
mmu-miR-365-1-5p_R1-22L23	AGGGACTTTTGGGGGCAGATGT	3.287378	1.716937	.039922
mmu-miR-3970_R1-15L20	TGAGGTTGTAGTTTGTACAGT	3.342656	1.740995	.049239
mmu-miR-409-3p	GAATGTTGCTCGGTGAACCCCT	6.67715	2.739232	.047799
mmu-miR-409-5p	AGGTTACCCGAGCAACTTTGCAT	3.15884	1.659395	.049728
mmu-miR-411-3p_R1-21L22	TATGTAACACGGTCCACTAACT	3.092754	1.628892	.042532
mmu-miR-450a-5p_R1-21L22	TTTTGCGATGTGTTCCTAATA	2.731815	1.44986	.047235
mmu-miR-486b-5p_R1-22L22	TCCTGTACTGAGCTGCCCCGAGTT	2.615984	1.387354	.018421
mmu-miR-503-3p_R1-21L22	GGAGTATTGTTTCCACTGCCTGA	4.637084	2.213218	.021239
mmu-miR-503-5p_R5-20L23	TAGAAGCGGGAACAGTACTG	2.512309	1.329014	.013754
mmu-miR-5121_R2-21L21	GCTTGTGATGAGACATCTCC	2.277513	1.187459	.036423
mmu-miR-542-3p_R1-18L22	TGTGACAGATTGATAACT	2.235336	1.160492	.04376
mmu-miR-547-3p_R4-21L21	CTGGGTACATCTTTGAGTGAG	2.006324	1.004554	.021002
mmu-miR-676-5p_R2-22L22	CTCTACAACCTTAGGACTTGC	2.81663	1.49397	.024758
mmu-miR-760-3p_R1-17L20	TCGGCTCTGGGTCTGTGG	2.008404	1.00605	.03554
mmu-miR-98-5p_R1-18L22	TGAGGTAGTAAGTTGTATAGTT	2.632703	1.396545	.044292
mmu-miR-99b-3p_R1-19L22	CAAGCTCGTGTCTGTGGGT	2.301011	1.202268	.039889
odi-let-7d_R1-16L22	TGAGGTAGTGGGTTGTGTGGTT	2.821886	1.496659	.008429
pma-miR-100b_R1-20L22	AACCCGTAGATTCGAACTTGT	2.410477	1.269319	.026821
pma-miR-4566_R18-4L22	GAACGTTGCACACTGCCAGATGGAAGTCCTT	2.099794	1.070248	.017057
ssa-miR-8156-5p_R15-1L21	TCCAGGACAGTCAGGACTATT	2.732164	1.450044	.019892
tch-miR-26a-2-5p_R1-20L22	TTCAAGTAACCCAGGATAGG	2.495726	1.31946	.001223
zma-miR2275c-5p_R21-7L21	CTTACGGACGTGAGGGTTCAAGTCCCTCTCTTC	4.311012	2.108026	.019223

Abbreviations: A, 2 Gy CIR exposure; CIR, carbon ion radiation; CK, control; miRNA, microRNA.

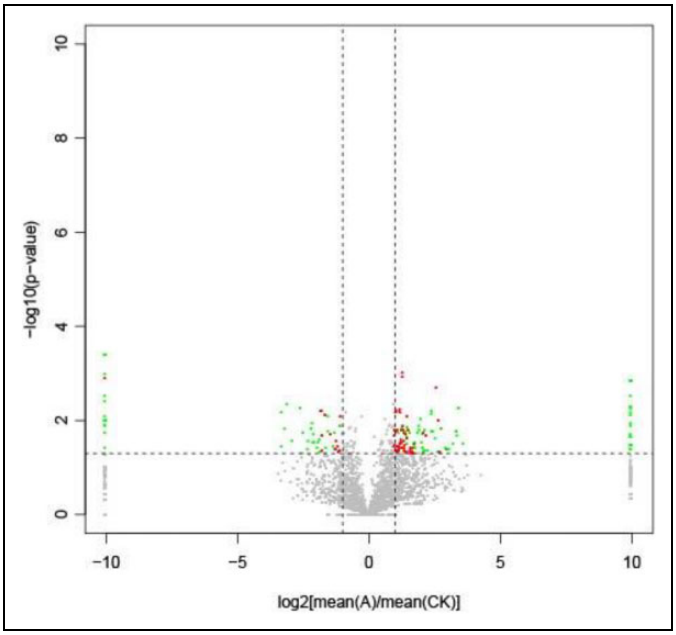

Figure 4. A volcano plot illustrates the height differentially expressed microRNAs (miRNAs) in mice testis at 4 weeks after carbon ion radiation (CIR), a criterion of $|\log2(\text{fold-change})| \geq 1$ and P value <.05 between the 2 groups was used to identify differentially expressed miRNAs. X-axis represents the $\log_2$ (fold change value), while y-axis represents −log10 (false discovery rate, FDR). Gray spots show no difference in expression. Green spots show the difference in expression based on the primary screening criteria ($|\log2(\text{fold-change})| \geq 1$ and P value <.05). Red spots show the difference in expression based on the high screening criteria ($|\log2(\text{fold-change})| \geq 1$ and P value <.05, at least the $|\log2(\text{fold-change})| \geq 1$ in one compared group).

Quantitative Reverse Transcription-Polymerase Chain Reaction Analysis

Based on KEGG results for the predicted target genes, we found that apoptosis plays an important role in spermatogenic cells in the testis following CIR exposure, indicating that this pathway may be related to reductions in testis weight and spermatogenic cell damage. Therefore, we used miRNAs involved in the apoptosis pathway to validate the quality of the sequencing results. The let-7 miRNA family members as well as miR-34c and miR-138 were reported in testis following IR exposure; therefore, we chose 6 upregulated let-7 miRNA family members (mmu-let-7a-5p_R1-22L22, mmu-let-7b-5p_R1-22L22, mmu-let-7c-5p_R1-22L22, mmu-let-7e-5p_R1-22L22, mmu-let-7f-5p_R1-22L22, and mmu-let-7i-5p_R4-22L22), as well as miR-34c and miR-138, and determined their expression by qRT-PCR analysis. The primers used are listed in Table 3, and the results of qRT-PCR are showed in Figure 8. Our results demonstrated that miR-34c and miR-138 were downregulated, and mmu-let-7a-5p_R1-22L22, mmu-let-7b-5p_R1-22L22, mmu-let-7c-5p_R1-22L22, mmu-let-7e-5p_R1-22L22, mmu-let-7f-5p_R1-22L22, and mmu-let-7i-5p_R4-22L22 were upregulated. These results agreed with those obtained by miRNA sequencing analysis (Tables 1 and 2).

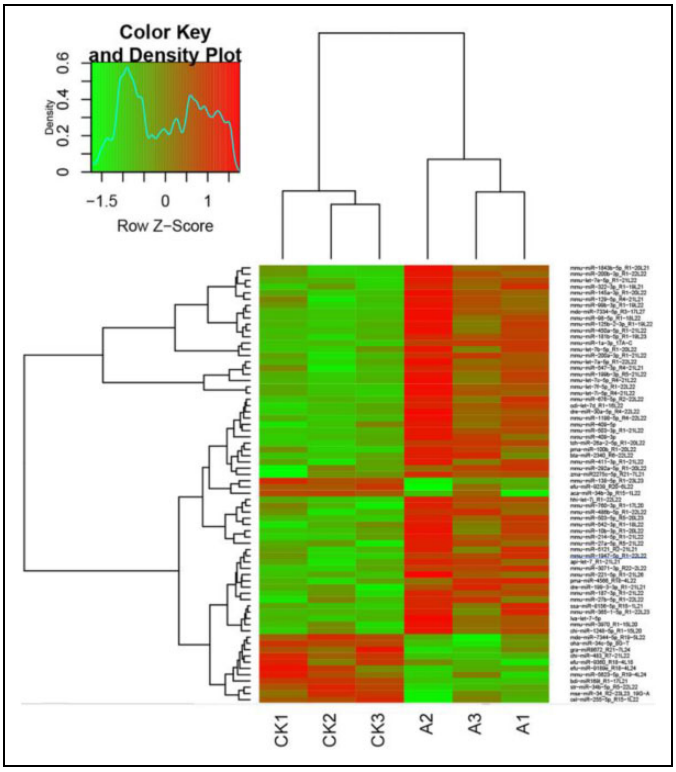

Figure 5. The differentially expressed microRNA (miRNA) in mice testis at 4 weeks after carbon ion radiation (CIR) profiles heatmap was constructed using mirPathv.3 Online Software. Red signals indicate downregulated expression and green signals indicate upregulated expression. A indicates 2 Gy CIR exposure; CK, control.

Discussion

Radiation treatment can induce apoptosis in germ cells, resulting in complete or temporary interruption of spermatogenesis. The testes are among the most sensitive organs to radiation due to the extreme sensitivity of highly mitotic, immature spermatogonia to radiation.[21] Understanding the regulatory role of miRNAs in the testes is important to the investigation of network-related mechanisms related to testicular injury following CIR exposure. The results of this study suggested that differentially expressed miRNAs directly or indirectly regulate testicular function following CIR exposure.

A model of radiation injury was developed based on radiation dosage and time following CIR exposure. We used a dose of 2 Gy, which was equivalent to the fractional radiation dose commonly used in patients,[22] followed by monitoring of essential reproductive indices at 1, 4, and 7 weeks following CIR exposure to simulate dynamic changes in the male reproductive system following CIR exposure. We then selected time points at which the most severe injury was observed before comparing changes in miRNA expression in mouse testis following 2 Gy CIR exposure. Testis injury was evaluated by comparing the relative weight of the testis, testicular histology, and the rate apoptosis in spermatogenic cells. Our results indicated that CIR exposure caused long-term damage to testis and spermatogenesis, and that this damage was most acute at 4 weeks after CIR

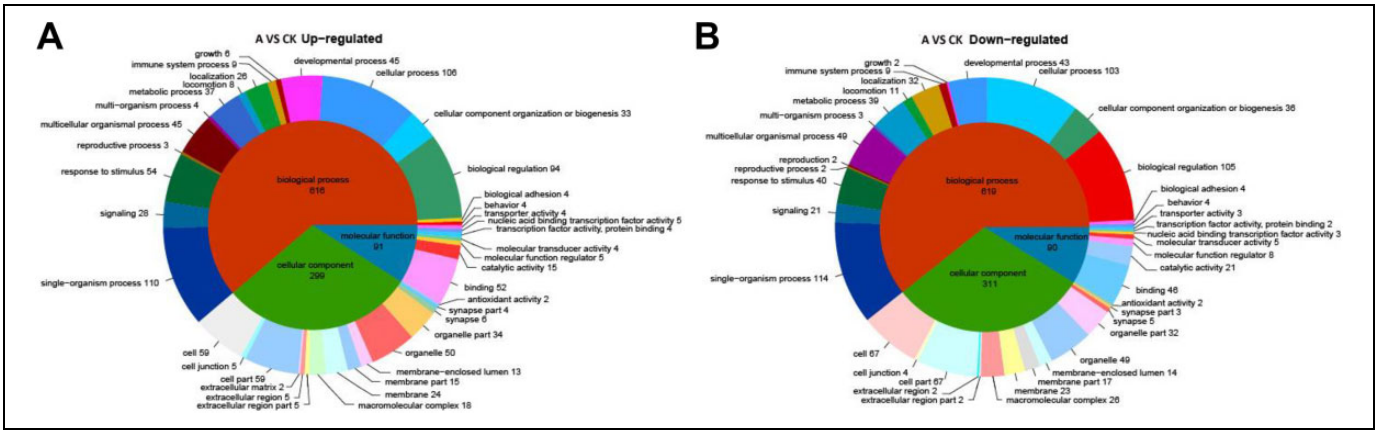

Figure 6. Gene ontology (GO) enrichment analysis of the differentially upregulated microRNA (miRNA; A) and the downregulated miRNA (B) in mice testis at 4 weeks after carbon ion radiation (CIR). A indicates 2 Gy CIR exposure; CK, control.

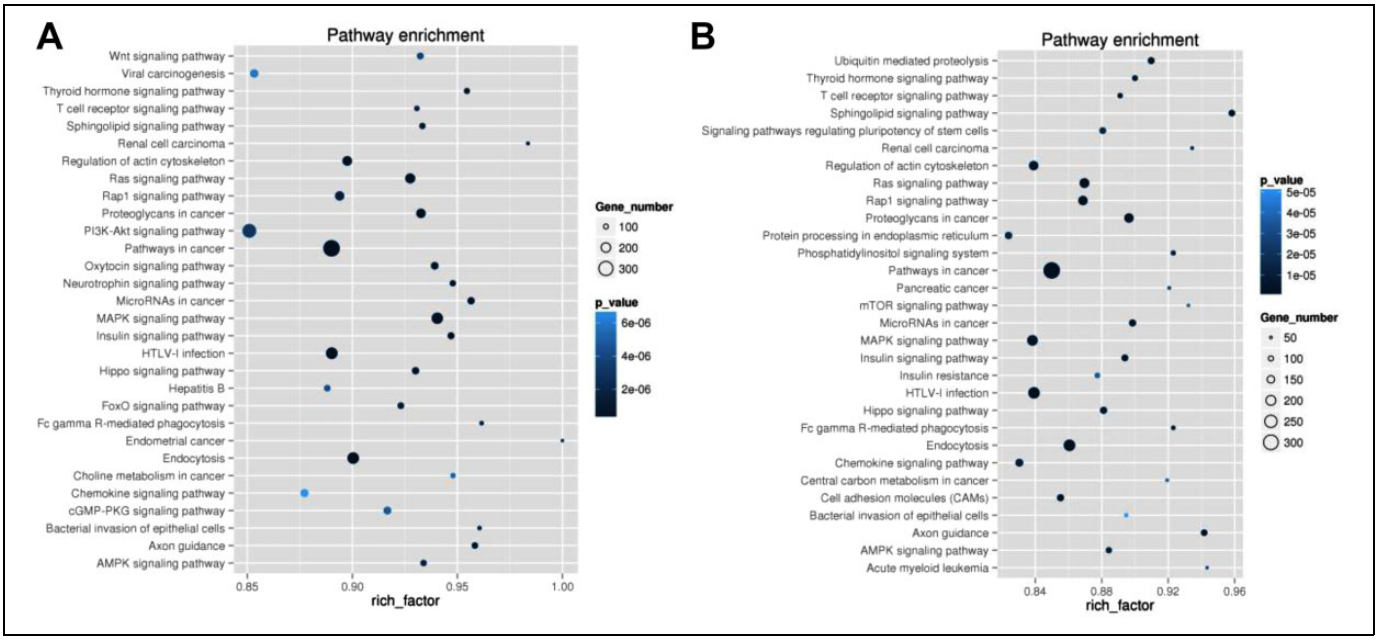

Figure 7. Pathway analysis of the target genes of differentially upregulated microRNA (miRNA; A) and the downregulated miRNA (B) in mice testis at 4 weeks after carbon ion radiation (CIR). A indicates 2 Gy CIR exposure; CK, control.

exposure. Therefore, this time point was chosen to investigate alterations in miRNA expression in mouse testis.

MiRNAs are involved in the regulation of gene expression and protein translation,[23] and due to miRNA stability, they can be easily detected and are considered as predictive tools and important intervention targets for many diseases.[24] Although previous studies reported changes in miRNA expression in testes following IR exposure, Khan et al demonstrated that 14 miRNAs were differentially expressed in mouse testis exposed to whole-body proton irradiation (2 Gy).[25] However, there were no studies investigating the role of miRNAs in spermatogenesis following CIR exposure. As important regulators of spermatogenesis and germ cell apoptosis, miRNAs might help explain the effects of CIR on testis function. In order to investigate changes in miRNA expression in testis after CIR exposure, we investigated miRNA expression profiles following irradiation (2 Gy) and compared to controls. We identified 70 differentially expressed miRNAs associated with multiple biological processes, including response to insulin, apoptosis, intracellular signaling cascades, and the inflammatory response. We then mapped differentially expressed miRNAs to specific gene targets to establish potential regulatory networks given that miRNA target genes can regulate cell development and differentiation, the cell cycle, and apoptosis as well as play important regulatory roles in cell biology.[26] To elucidate the function of miRNA targets, KEGG pathway and GO analyses were performed on the target genes. Radiation may disrupt the balance between spermatogenic cell proliferation and apoptosis, and excessive apoptosis of spermatogenic cells

Table 3. The Primers of Each Selected miRNA.

miRNA	Loop Primer/F Primer
mmu-let-7a-5p	5′-GTCGTATCCAGTGCAGGGTCCGAGGTA TTCGCACTGGATACGACAACTATAC/ TGCGCTGAGGTAGTAGGTTGTA
mmu-let-7b-5p	5′-GTCGTATCCAGTGCAGGGTCCGAGGTA TTCGCACTGGATACGACAACCACAC/ TGCGCTGAGGTAGTAGGTTGTG
mmu-let-7c-5p	5′-GTCGTATCCAGTGCAGGGTCCGAGGTA TTCGCACTGGATACGACAACCATAC/ TGCGCTGAGGTAGTAGGTTGTA
mmu-let-7e-5p	5′-GTCGTATCCAGTGCAGGGTCCGAGGTA TTCGCACTGGATACGACAACTATAC/ TGCGCTGAGGTAGGAGGTTGTA
mmu-let-7f-5p	5′-GTCGTATCCAGTGCAGGGTCCGAGGTA TTCGCACTGGATACGACAACTATAC/ TGCGCTGAGGTAGTAGATTGTA
mmu-let-7i-5p	5′-GTCGTATCCAGTGCAGGGTCCGAGGT ATTCGCACTGGATACGACAACAGCAC/ TGCGCTGAGGTAGTAGTTTGTG
oha-miR-34c-5p	5′-GTCGTATCCAGTGCAGGGTCCGAGGTA TTCGCACTGGATACGACACAATCAG/ TGCGCAGGCAGTGTAGTTAGCTG
mmu-miR-138-5p	5′-GTCGTATCCAGTGCAGGGTCCGAGGT ATTCGCACTGGATACGACCGGCCTGA/ TGCGCAGCTGGTGTTGTGAATCA

Abbreviation: miRNA, microRNA.

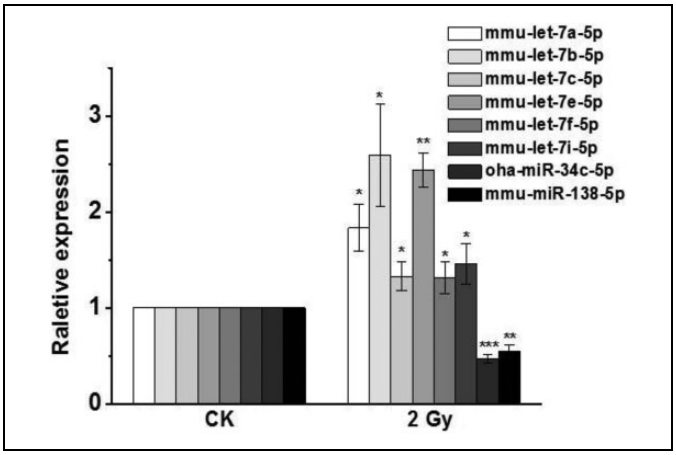

Figure 8. Relative expression of 8 selected microRNA (miRNA) was quantified by quantitative reverse transcription-polymerase chain reaction (qRT-PCR). Values represent averages ± SEM. Asterisks denote values that are different from controls: *$P < .05$, **$P < .01$, and ***$P < .001$ with Student *t* test analysis.

might induce spermatogenic disorders related to male infertility.[27] Wang et al found that CIR exposure induced spermatogenic cell apoptosis.[28] Here, we focused on the apoptosis pathway to validate the roles of differentially expressed miRNAs. Deep sequencing and qRT-PCR validated that the expression levels of identified miRNAs between irradiated mice testis and controls were largely consistent with sequencing analysis.

miR-34c is preferentially expressed in spermatogonial stem cell-enriched populations and is highly expressed in spermatocytes and round spermatids.[29,30] Inhibition of miR-34c in primary spermatocytes prevent germ cells from testosterone-deprivation-induced apoptosis.[31] miR-34c-5p levels in the testis from asthenozoospermic or oligoasthenozoospermic patients differed from those observed in normozoospermic men.[32] In this study, downregulation of miR-34c-5p prevented spermatogenic cells proliferation and induced apoptosis in spermatogenic cells following CIR exposure. miR-138 plays various roles in a variety of cancers[33] and negative regulation of anti-mullerian hormone (AMH). Additionally, elevated temperatures induce masculinization in Nile tilapia, during which miR-138 expression increased rapidly.[34,35] Furthermore, decreased miRNA expression promotes testicular differentiation by decreasing AMH levels in testes.[36] Hu et al found that miR-138 was downregulated in response to 17α-E2 treatment in mouse testicular Leydig tumor cells. Here, miR-138 downregulation suggested that decreased miR-138 expression promoted spermatogenic cell differentiation,[37] because IR exposure increased spermatogenic cell apoptosis and enhanced proliferation to maintain dynamic balance in testis.[38] The let-7 miRNA family is involved in the differentiation of spermatogonia from undifferentiated spermatogonia to A1 spermatogonia,[39] and let-7 miRNAs regulate the differentiation of spermatogonia by regulating IGF-1 signal pathway.[40] High-throughput sequencing revealed that 10 let-7 family members are present in channel catfish.[41] Mirlet7 family miRNAs are involved in retinoic acid-induced spermatogonial differentiation and are mainly expressed in spermatogonia and spermatocytes. We show that Mirlet7c, strongly expressed in the testis and spermatocyte stage, may be involve in regulating several distinct steps during spermatogenesis.[42] In this study, results of miRNA sequencing and qRT-PCR analysis revealed upregulation of 6 let-7 family members, consistent with results reported by Wang, showing significant upregulation of mmu-let-7d in response to proton radiation in mouse testis. These results agreed with a variety of previously observed changes in let-7 family members upon exposure to radiation.

To our knowledge, this study is the first to investigate the role of miRNA expression in mouse testes following CIR exposure. Differentially expressed miRNAs can provide novel insights into mechanisms related to testicular damage, although differentially expressed miRNAs are not key to testicular injury and may not participate in the same processes in humans. Therefore, miRNA and targeted gene studies should be performed in human cells or samples to confirm the results presented here.

Conclusions

In summary, the expression of multiple miRNAs was altered in mouse testes following CIR exposure, indicating that testicular damage may be due to changes in the expression of several of the identified miRNAs. Additionally, our results suggested that miRNAs might be potential biomarkers of testicular damage.

The results of this study provided insight into the potential contribution of miRNA regulation of testicular function and may promote development of prenatal diagnostic biomarkers for testis.

Authors' Note

Y.H. and Y.Z. contributed equally to this work.

Declaration of Conflicting Interests

The author(s) declared no potential conflicts of interest with respect to the research, authorship, and/or publication of this article.

Funding

The author(s) disclosed receipt of the following financial support for the research, authorship, and/or publication of this article: This research was supported by the National Natural Science Foundation of China (11505244), the the Western Talent Program of the Chinese Academy of Sciences (Y560020XB0), the Special Foundation for Talents of Gansu Agricultural University (2017RCZX-13), the National High Technology Research and Development Program of China (2013AA102505), and the Ministry of Science and Technology National Key R&D project (2016YFC0904600).

References

1. Silva AM, Correia S, Casalta-Lopes JE, et al. The protective effect of regucalcin against radiation-induced damage in testicular cells. *Life Sci*. 2016;164:31-41.
2. Shaha C, Tripathi R, Mishra DP. Male germ cell apoptosis: regulation and biology. *Philos Trans R Soc Lond B Biol Sci*. 2010; 365(1546):1501-1515.
3. Khan S, Adhikari JS, Rizvi MA, Chaudhury NK. Radioprotective potential of melatonin against 60 Co γ-ray-induced testicular injury in male C57BL/6 mice. *J Biomed Sci*. 2015;22(1):61.
4. Ding J, Wang H, Wu ZB, Zhao J, Zhang S, Li W. Protection of murine spermatogenesis against ionizing radiation-induced testicular injury by a green tea polyphenol. *Biol Reprod*. 2015;92(1):6.
5. Trost LW, Brannigan RE. Oncofertility and the male cancer patient. *Curr Treat Options Oncol*. 2012;13(2):146-160.
6. Li H, He Y, Zhang H, Miao G. Differential proteome and gene expression reveal response to carbon ion irradiation in pubertal mice testes. *Toxicol Lett*. 2014;225(3):433-444.
7. Dillon KE, Gracia CR. Pediatric and young adult patients and oncofertility. *Curr Treat Options Oncol*. 2012;13(2):161-173.
8. Krämer M, Scholz M. Treatment planning for heavy-ion radiotherapy: calculation and optimization of biologically effective dose. *Phys Med Biol*. 2000;45(11):3319-3330.
9. Ohno T. Particle radiotherapy with carbon ion beams. *EPMA J*. 2013;4(1):9.
10. Gu S, Kay MA. How do miRNAs mediate translational repression? *Silence*. 2010;1:11.
11. Bajan S, Hutvagner G. Regulation of miRNA processing and miRNA mediated gene repression in cancer. *Microrna*. 2014; 3(1):10-17.
12. Riemondy K, Hoefert JE, Yi R. Not miR-ly micromanagers: the functions and regulatory networks of miRNAs in mammalian skin. *Wiley Interdiscip Rev RNA*. 2014;5(6):849-865.
13. Tang D, Huang Y, Liu W, Zhang X. Up-regulation of microRNA-210 is associated with spermatogenesis by targeting IGF2 in male infertility. *Med Sci Monit*. 2016;22:2905-2910.
14. Noveski P, Popovska-Jankovic K, Kubelka-Sabit K, et al. MicroRNA expression profiles in testicular biopsies of patients with impaired spermatogenesis. *Andrology*. 2016;4(6):1020-1027.
15. Li H, He Y, Yan J, Zhao Q, Di C, Zhang H. Comparative proteomics reveals the underlying toxicological mechanism of low sperm motility induced by iron ion radiation in mice. *Reprod Toxicol*. 2016;65:148-158.
16. Li H, Zhang H, Di C, et al. Comparative proteomic profiling and possible toxicological mechanism of acute injury induced by carbon ion radiation in pubertal mice testes. *Reprod Toxicol*. 2015; 58:45-53.
17. Li C, Chen L, Zhao Y, et al. Altered expression of miRNAs in the uterus from a letrozole-induced rat PCOS model. *Gene*. 2016;598: 20-26.
18. Yang H Lin S, Lei X, et al. Identification and profiling of microRNAs from ovary of estrous Kazakh sheep induced by nutritional status in the anestrous season. *Anim Reprod Sci*. 2016;175:18-26.
19. Tse AC, Li JW, Wang SY, Chan TF, Lai KP, Wu RS. Hypoxia alters testicular functions of marine medaka through microRNAs regulation. *Aquat Toxicol*. 2016;180:266-273.
20. Liu Z, Jiang H, Yang J, et al. Analysis of altered microRNA expression profiles in the kidney tissues of ethylene glycol-induced hyperoxaluric rats. *Mol Med Rep*. 2016;14(5):4650-4658.
21. Osterberg EC, Ramasamy R, Masson P, Brannigan RE. Current practices in fertility preservation in male cancer patients. *Urol Ann*. 2014;6(1):13-17.
22. Tharavichtikul E, Meungwong P, Chitapanarux T, et al. The association of rectal equivalent dose in 2 Gy fractions (EQD2) to late rectal toxicity in locally advanced cervical cancer patients who were evaluated by rectosigmoidoscopy in Faculty of Medicine. *Radiat Oncol J*. 2014;32(2):57-62.
23. Shuo G, Mark AK. How do miRNAs mediate translational repression? *Silence*. 2010;1:11.
24. Xiaoli Z, Yawei W, Lianna L, Haifeng L, Hui Z. Screening of target genes and regulatory function of miRNAs as prognostic indicators for prostate cancer. *Med Sci Monit*. 2015;21: 3748-3759.
25. Khan SY, Tariq MA, Perrott JP, et al. Distinctive microRNA expression signatures in proton-irradiated mice. *Mol Cell Biochem*. 2013;382(1-2):225-235.
26. Mathieu J, Ruohola-Baker H. Regulation of stem cell populations by microRNAs. *Adv Exp Med Biol*. 2013;786:329-351.
27. Li HY, Zhang H. Proteome analysis for profiling infertility markers in male mouse sperm after carbon ion radiation. *Toxicology*. 2013;306:85-92.
28. Wang B, Murakami M, Eguchi-Kasai K. Effects of prenatal irradiation with accelerated heavy-ion beams on postnatal development in rats: III. Testicular development and breeding activity. *Adv Space Res*. 2007;40(4):550-562.
29. Bouhallier F, Allioli N, Lavial F, et al. Role of miR-34c microRNA in the late steps of spermatogenesis. *RNA*. 2010;16(4): 720-731.

30. Tan T, Zhang Y, Ji W, Zheng P. miRNA signature in mouse spermatogonial stem cells revealed by high-throughput sequencing. *Biomed Res Int*. 2014;2014:154251.
31. Liang X, Zhou D, Wei C, et al. MicroRNA-34c enhances murine male germ cell apoptosis through targeting ATF1. *PLoS One*. 2012;7(3):e33861.
32. Wang C, Yang C, Chen X, Yao B, Yang C. Altered profile of seminal plasma microRNAs in the molecular diagnosis of male infertility. *Clin Chem*. 2011;57(12):1722-1731.
33. Yang H, Tang Y, Guo W, et al. Up-regulation of microRNA-138 induce radiosensitization in lung cancer cells. *Tumour Biol*. 2014; 35(7):6557-6565.
34. Poonlaphdecha S, Pepey E, Canonne M, de Verdal H, Baroiller JF, D'Cotta H. Temperature induced-masculinisation in the Nile tilapia causes rapid up-regulation of both dmrt1 and amh expressions. *Gen Comp Endocrinol*. 2013;193: 234-242.
35. Eshel O, Shirak A, Dor L, Band M, Zak T, Markovich-Gordon M. Identification of male-specific amh duplication, sexually differentially expressed genes and microRNAs at early embryonic development of Nile tilapia (Oreochromis niloticus). *BMC Genomics*. 2014;15:774.
36. Wang W, Liu W, Liu Q, et al. Coordinated microRNA and messenger RNA expression profiles for understanding sexual dimorphism of gonads and the potential roles of microRNA in the steroidogenesis pathway in Nile tilapia (Oreochromis niloticus). *Theriogenology*. 2016;85(5):970-978.
37. Hu Z, Shen WJ, Cortez Y, et al. Hormonal regulation of microRNA expression in steroid producing cells of the ovary. Testis and adrenal gland. *PLoS One*. 2013;8(10):e78040.
38. Li HY, Zhang H, Miao GY, et al. Simulated microgravity conditions and carbon ion irradiation induce spermatogenic cell apoptosis and sperm DNA damage. *Biomed Environ Sci*. 2013;26(9): 726-734.
39. Tong MH, Mitchell DA, McGowan SD, Evanoff R, Griswold MD. Two miRNA clusters, Mir-17-92 (Mirc1) and Mir-106b-25 (Mirc3), are involved in the regulation of spermatogonial differentiation in mice. *Biol Reprod*. 2012;86(3):72.
40. Shen G, Wu R, Liu B, et al. Upstream and downstream mechanisms for the promoting effects of IGF-1 on differentiation of spermatogonia to primary spermatocytes. *Life Sci*. 2014;101(1-2): 49-55.
41. Xu Z, Chen J, Li X, Ge J, Pan J, Xu X. Identification and characterization of MicroRNAs in channel catfish (Ictalurus punctatus) by using solexa sequencing technology. *PLoS One*. 2013; 8(1):e54174.
42. Tong MH, Mitchell D, Evanoff R, Griswold MD. Expression of Mirlet7 family microRNAs in response to retinoic acid-induced spermatogonial differentiation in mice. *Biol Reprod*. 2011;85(1): 189-197.